Effect of Monomers on the Basal Spacing of Sodium Montmorillonite and the Structures of Polymer−Clay Nanocomposites

Yeong Suk Choi, Hyeong Taek Ham, and In Jae Chung*

Department of Chemical and Biomolecular Engineering, Korea Advanced Institute of Science and Technology, 373-1, Guseong-dong, Yuseong-gu, Daejeon, Korea

Received September 15, 2003. Revised Manuscript Received April 16, 2004

The basal spacings of sodium montmorillonite (MMT) dispersed in various solvents and monomers were measured via X-ray diffraction. Some liquids with strong hydrogen-bonding groups (δ_h) showed little suspended MMT, but liquids with moderate or poor hydrogen-bonding groups precipitated MMT completely, this indicates that δ_h is an important factor for the dispersion state of natural MMT in a liquid. The basal spacing expansion also depends on polar components (δ_p) and hydrogen-bonding components (δ_h) of organic liquids. Liquids with high δ_h values showed expansion in the order of methyl alcohol > ethyl alcohol > 2-propyl alcohol > *n*-hexane > toluene > benzene, and monomers with high δ_p values exhibited expansion in the order of *n*-butyl acrylate > acrylonitrile > methyl methacrylate > styrene. Because dipole−dipole interactions involved both δ_h and δ_p, liquid dipole moments were adopted to explain the expansion of MMT in polymer−MMT nanocomposites. Monomers with high dipole moments showed large basal spacings before polymerization and produced exfoliated polymer−MMT nanocomposites, whereas those with low dipole moments showed smaller basal spacings and produced intercalated polymer−MMT nanocomposites.

Introduction

Intensive research on polymer−clay nanocomposites in organic−inorganic hybrids is important because clay nanocomposites have a high modulus, dimensional stability, low gas permeability, and flame retardation through self-extinguishing behavior.[1−14] These enhanced properties result from nanoscale dispersions in polymer matrixes and the subsequent interaction between the clays and the polymers.

Recently, Hansen solubility parameters, $\delta_t^2 = \delta_d^2 + \delta_p^2 + \delta_h$, were used to explain the dispersion of organically modified clays (organoclays) in organic solvents.[15−19] The dispersive components of the solvents (δ_d) greatly affected the degree of dispersion because of the hydrophobic modifier molecules that covered the organoclays. The polar components (δ_p) and the hydrogen components (δ_h) are important for the dispersion or exfoliation of natural clays. If natural clays are used to produce polymer−clay nanocomposites, the molecular sizes of the intercalants give in situ polymerizations an advantage over the melt intercalation method and the solution intercalation method because the intercalants of in situ polymerization such as monomers or precursors can penetrate the interlayer spaces of the clays more easily than polymers or macromolecules.

Smectite clays have the properties of cation exchange, intercalation of molecules, and swelling in solvents.[20] Their swelling capacity as a cation exchanger is fundamental to their intercalation and swelling properties. Alkylammoniums or metal cations can displace hydrated cations on the clay layers by exchanging ions. Smectite clays can imbibe metal ions or neutral molecules. For example, sodium montmorillonite (MMT), which is a type of smectite clay, expands the interlayer spaces when immersed in a hydrophilic solvent such as water. The adsorption of organic molecules by natural clays depends on the physical and chemical properties

* To whom correspondence should be addressed. Tel.: 82-42-869-3916. Fax: 82-42-869-3910. E-mail: chung@kaist.ac.kr.

(1) Vaia, R. V.; Teukolsky, R. K.; Giannelis, E. P. *Chem. Mater.* **1994**, *6*, 1017.
(2) Lan, T.; Kaviratna, P. D.; Pinnavaia, T. J. *Chem. Mater.* **1994**, *6*, 573.
(3) Lan, T.; Pinnavaia, T. J. *Chem. Mater.* **1994**, *6*, 2216.
(4) Lan, T.; Kaviratna, D.; Pinnavaia, T. J. *J. Phys. Chem. Solids* **1996**, *57*, 1005.
(5) Haraguchi, K.; Takehisa, T.; Fan, S. *Macromolecules* **2002**, *35*, 10162.
(6) Hoffmann, B.; Dietrich, C.; Thomann, R.; Friedrich, C.; Mülhaupt, R. *Macromol. Rapid Commun.* **2000**, *21*, 57.
(7) Becker, O.; Cheng, Y. B.; Varley, R. J.; Simon, G. P. *Macromolecules* **2003**, *36* (5), 1616.
(8) Tarasevich, Y. I.; Aksenenko, E. V. *Colloids Surf., A* **2001**, *180*, 33.
(9) Byun, H. Y.; Choi, M. H.; Chung, I. J. *Chem. Mater.* **2001**, *13*, 4221.
(10) Choi, Y. S.; Wang, K. H.; Xu, M.; Chung, I. J. *Chem. Mater.* **2002**, *14*, 2936.
(11) Choi, Y. S.; Choi, M. H.; Wang, K. H.; Kim, S. O.; Kim, Y. K.; Chung, I. J. *Macromolecules* **2001**, *34*, 8978.
(12) Kim, Y. K.; Choi, Y. S.; Wang, K. H.; Chung, I. J. *Chem. Mater.* **2002**, *14*, 4990.
(13) Pinnavaia, T. J.; Beall, G. W. *Polymer-Clay Nanocomposites*; John Wiley & Sons: New York, 2001.
(14) Shonaike, G. O.; Advani, S. G. *Advanced Polymeric Materials: Structure Property Relationships*; CRC Press: Boca Raton, FL, 2003.
(15) Ho, D. L.; Glinka, C. J. *Chem. Mater.* **2003**, *15*, 1309.
(16) Ho, D. L.; Briber, R. M.; Glinka, C. J. *Chem. Mater.* **2001**, *13*, 1923.
(17) Hansen, C. M. *J. Paint Technol.* **1967**, *39*, 104.
(18) Brandrup, J.; Immergut, E. H. *Polymer Handbook*, 4th ed.; Wiley: New York, 1999.
(19) Barton, A. F. M. *CRC Handbook of Solubility Parameters and Other Cohesion Parameters*; CRC Press: Boca Raton, FL, 1991.
(20) Pinnavaia, T. J. *Science* **1983**, *220*, 4595.

10.1021/cm0348601 CCC: $27.50
Published on Web 05/26/2004

of the clay. If the organic molecules react strongly with the hydrophilic clays, the clay layers strongly attract the molecules.[21−29]

To produce exfoliated polymer−clay nanocomposites, we therefore need to understand and use the interactions between the clay surfaces and the intercalants. Organic molecules can penetrate the spaces between the layers of the clay by interacting with the clay surface in the following ways:[30](i) cationic bonding, in which the protonated alkylammoniums replace the sodium ions in MMT layers, (ii) ion−dipole interactions, in which the polar organic molecules are related to the sodium ions in the MMT layers, and (iii) dipole−dipole interactions, which include the hydrogen bonding that associates polar organic molecules with hydroxyl groups or oxygen in the clay layers.

We used a surfactant that had ionic groups which replaced the sodium ions, though we did not consider cationic bonding because the quantity of the surfactant was fixed for all experiments. As a result, of all the interactions, the dipolar interactions were the most significant. To investigate the degree of the interactions, we used the dipole moments of the monomers because most vinyl monomers have pendant groups that are capable of dipolar interactions or van der Waals interactions with the layers of clay.

We used organic solvents and monomers to examine the MMT basal spacing, or d_{001}-spacing.[31] Through this examination, we determined that the basal spacing expansion by monomers is related to the monomer dipole moments and to the structures of polymer−MMT nanocomposites.[32] To compare the dipole moment values, we selected four monomers (acrylonitrile (AN), *n*-butyl acrylate (BA), methyl methacrylate (MMA), and styrene) and mixed monomers (BA, styrene, and MMA). We then synthesized the polymer−clay nanocomposites through a semi-batch emulsion polymerization method.[33]

Experimental Section

Materials. Methyl alcohol (MeOH), ethyl alcohol (EtOH), 2-propyl alcohol (IPA), *n*-hexane, benzene, and toluene were purchased from Merck and used as received. AN, BA, MMA, styrene, dodecylbenzenesulfonic acid sodium salt (DBS−Na), and 2-acrylamido-2-methyl-1-propanesulfonic acid (AMPS)[10−12] were purchased from Aldrich and were used as received. The Kunimine Co. supplied the Kunipia-F MMT for this experiment; it had 119 mequiv for each 100 g of cation exchange capacity. Potassium persulfate (KPS), a radical initiator purchased from Junsei Chemical Co., was recrystallized using deionized water.

Preparation of Clay Dispersion in Liquids. We added 3 g of pristine MMT to an Erlenmeyer flask containing 30 g of a liquid (monomer or solvent), and closed the neck opening with a plug-seal screw cap. The amount of liquid was much greater than the cationic exchange capacity of the MMT. To examine the dispersion state of the liquid−MMT by turbidity, we stirred it for 48 h at 300 rpm at room temperature, and then let it rest for 24 h. Most clay particles settled on the bottom of the flask. We placed the MMT sediment on a grooved glass holder to measure the basal spacing of MMT using X-ray diffraction (XRD), and obtained the XRD peak under the same condition as the polymer−clay nanocomposites.

Synthesis of Polymer−Clay Nanocomposites. Before polymerization, we dispersed 5 g of pristine MMT in 145 g of deionized water for 24 h at ambient temperature. We then synthesized various polymer−clay nanocomposites, excluding poly(BA) (PBA) and PBA copolymer−clay nanocomposites, via the semi-batch emulsion polymerization described elsewhere.[10−12] To produce PBA, poly(BA-*co*-MMA) (P(BA-*co*-MMA)), and poly(BA-*co*-styrene) (P(BA-*co*-S)), we used the following ingredients in the initial stage under a polymerization temperature of 75 °C: monomer (5 g), AMPS (0.3 g), water (120 g), and an initiator aqueous solution (4 g/1 wt %). After the initial stage, we charged 15 g of monomer at a rate of 0.2 cm^3/min in the incremental stage. To stabilize the P(BA-*co*-S)−MMT nanocomposites after the initial stage, we added 1 g of aqueous DBS−Na solution (10 wt %). To avoid the AMPS effect on the polymerization rates, we fixed the amount of AMPS in the initial stage to 0.3 g.

Measurements. We used a Rigaku X-ray generator (Cu Kα with $\lambda = 0.15406$ nm) at room temperature to obtain XRD peaks with a scanning rate of 2°/min in the 2θ range of 1.2° to 10°. After molding the nanocomposites into a disk shape under 3000 psi, we obtained the XRD patterns for the final polymer−MMT nanocomposites.

To record the Fourier transform infrared (FT-IR) spectra, we used a BIO-RAD FTS 3000 FT-IR spectrometer equipped with a GRASEBY SPECAC diamond-attenuated total reflectance. We took an average of 40 scans at 4 cm^{-1} of resolution. To sustain the samples, we fitted the cover of the diamond-attenuated total reflectance to reach the bottom glass.

Proton nuclear magnetic resonance (^{1}H NMR) spectra were recorded on a Bruker DRX 300 NMR spectrometer. We used dimethyl sulfoxide (DMSO, $(CD_3)_2SO$) to determine the monomer ratio in the basal spacing before the polymerization, and we used a glass syringe to insert liquid−MMT into a medium bottle. The liquid in the bottle was drained with a syringe until the liquid no longer seeped out of the MMT sediment. The MMT sediment was dried for 1 h at room temperature. To extract the monomer, we added 100 μL of DMSO to the MMT sediment and then sonicated the sediment for 10 h. We filtered the DMSO with a 0.45-μm syringe filter from Whatman and added it to an NMR tube. To determine the composition of the end-tethered copolymers recovered by a reverse-ion-exchange method we used acetone (CD_3COCD_3) and deuterium oxide (D_2O), mixed at a 1:1 volume ratio.[10−12]

A Philips CM-20 transmission electron microscope (TEM) was used to examine the morphology of the nanocomposite. After molding the nanocomposite with epoxy, we sliced it to a thickness of 70 nm with a Boeckeler CRX cyro-ultramicrotome at the temperature of liquid nitrogen. The accelerating voltage of the TEM was 160 kV.

Results

Hansen derived the most widely used solubility parameters from the Hildebrand solubility parameters.[17] The Hansen solubility parameters consist of three components: the dispersive component (δ_d), the polar component (δ_p), and the hydrogen bonding component (δ_h). The equation is expressed as $\delta_t^2 = \delta_d^2 +$

(21) Blumstein, A. *J. Polym. Sci. A.* **1965**, *3*, 2653.
(22) Blumstein, A.; Billmeyer, F. W., Jr. *J. Polym. Sci., Part A-2* **1966**, *4*, 465.
(23) Blumstein, A.; Parikh, K. K.; Malhotra, S. L. *J. Polym. Sci., Part A-2* **1971**, *9*, 1681.
(24) Kato, C.; Kuroda, K.; Misawa, M. *Clays Clay Miner.* **1979**, *27*, 129.
(25) Newsham, M. D.; Giannelis, E. P.; Pinnavaia, T. J. *J. Am. Chem. Soc.* **1988**, *110*, 3885.
(26) Kinrade, S. D.; Nin, J. W. D.; Schach, A. S.; Sloan, T. A.; Wilson, K. L.; Knight, C. T. G. *Science* **1999**, *285*, 1542.
(27) Kojima, Y.; Usuki, A.; Kawasumi, M.; Okada, A.; Fukushima, Y.; Kurauchi, T.; Kamigaito, O. *J. Mater. Res.* **1993**, *8*, 1185.
(28) Murry, H. H. *Appl. Clay Sci.* **2000**, *17*, 207.
(29) Lagaly, G. *Appl. Clay Sci.* **1999,** *17*, 207.
(30) Giese, R. F.; van Oss, C. J. *Colloid and Surface Properties of Clays and Related Minerals*; Marcel Dekker: New York, 2002.
(31) Vaia, R. A.; Liu, W. *J. Polym. Sci. Polym. Phys.* **2002**, *40*, 1590.
(32) Blackley, D. C. *Emulsion Polymerization Theory and Practice*; Science Publishers Ltd: Essex, England, 1982.
(33) Ride, R. D. *CRC Handbook of Chemistry and Physics*, 81st ed.; CRC Press: Boca Raton, FL, 2000−2001.

Table 1. Dispersion States of MMT in Various Liquids and the Hansen Solubility Parameters[a]

organic liquids[18]	δ_d MPa$^{1/2}$	δ_p MPa$^{1/2}$	δ_h MPa$^{1/2}$	δ_t[b] MPa$^{1/2}$	H-bonding group[c]	dispersion state
water	15.5	16.0	42.4	47.9	s	viscous paste
methyl alcohol (MeOH)	15.1	12.3	22.3	29.7	s	slightly suspended
ethyl alcohol (EtOH)	15.8	8.8	19.4	26.6	s	slightly suspended
2-propyl alcohol (IPA)	15.8	6.1	16.4	23.5	s	slightly suspended
n-butyl acrylate (BA)[19]	14.0	8.3	6.8	17.7	m	precipitated
methyl methacrylate (MMA)[19]	13.7	9.8	6.1	17.9	m	precipitated
acrylonitrile (AN)	16.5	17.4	6.8	24.8	p	precipitated
styrene	18.6	1.0	4.1	19.0	p	precipitated
benzene	18.4	0	2.0	18.6	p	precipitated
toluene	18.0	1.4	2.0	18.2	p	precipitated
n-hexane	14.9	0	0	14.9	p	precipitated

[a] All solubility parameter values are from refs 18 and 19 and the unit is MPa$^{1/2}$. [b] $\delta_t^2 = \delta_d^2 + \delta_p^2 + \delta_h^2$, where δ_t is the total (or Hildebrand) solubility parameter, δ_d is the dispersive component, δ_p is the polar component, and δ_h is the hydrogen-bonding component of the Hansen solubility parameters. [c] The parameters s, m, and p in the H-bonding group column stand for strong, moderate, and poor, which were classified by ref 18.

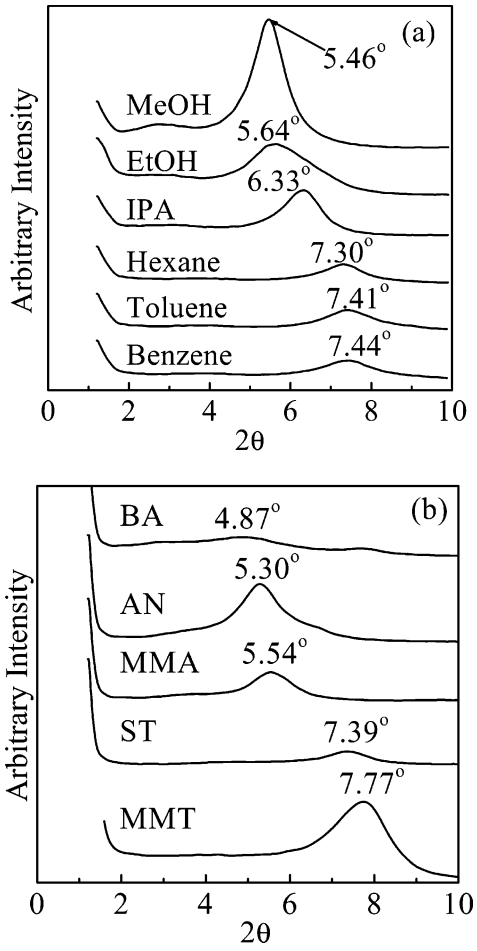

Figure 1. XRD patterns of liquid−MMT with a weight ratio of 30:3 for (a) organic solvents and (b) vinyl monomers. The pattern of MMT was measured at its dry state.

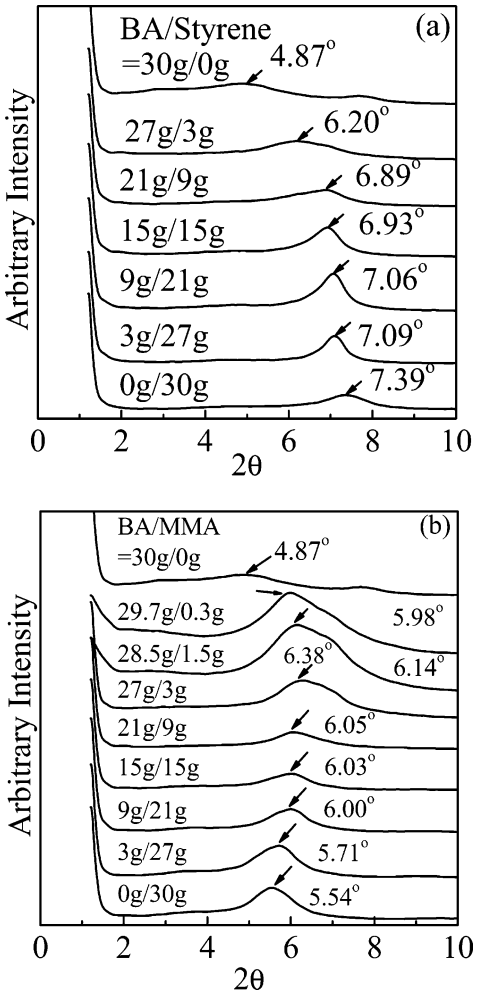

Figure 2. XRD patterns of (a) BA−styrene−MMT dispersions and (b) BA−MMA−MMT dispersions with a weight ratio of 30:3.

$\delta_p^2 + \delta_h^2$, $\delta_t = (E/V)^{1/2}$, where δ_t is the total (or Hildebrand) solubility parameter, E is the vaporization energy of a solvent, and V is the molar volume of a solvent.

These three components can explain the mixing behavior of polar solvents or polymers. However, before we can explain the dispersion states of MMT in organic liquids, we must allude to a few aspects of the Hansen solubility parameters.[18,19] For example, the total solubility parameter (δ_t) of an MMT layer whose diameter is less than 2 μm is so high that an MMT layer is not miscible or soluble in organic liquids, monomers, or polymers. Furthermore, although the total solubility parameters (δ_t) of the liquids are almost the same, the liquids interact differently with MMT because they have different component values in the Hansen solubility parameters.

Table 1 shows the dispersion states of MMT in various liquids and the Hansen solubility parameters. When we put MMT in water, the water−MMT quickly became a viscous paste because the MMT layer was very hydrophilic. Over 24 h, the three solvents MeOH, EtOH, and

Table 2. Monomer Dipole Moments and Basal Spacing of MMT after Monomer Adsorption

monomers and feed weights (abbreviation of monomer)	molar ratio of feed monomer[a]	molar ratio of monomer in d_{001} space[b]	peak position (2θ)	d_{001} space (nm)	gap size of MMT (nm)[c]	dipole moment (D)
n-butyl acrylate (BA)	100	100	4.87	1.81	0.85	2.31[d]
BA/MMA 29.7:0.3	100/1.3	100/1.3	5.98	1.48	0.52	
BA/MMA 28.5:1.5	100/6.7	100/5.9	6.14	1.44	0.48	
BA/MMA 27:3	100/14.3	100/13.1	6.38	1.39	0.43	
BA/MMA 21:9	100/54.9	100/54.1	6.05	1.46	0.5	
BA/MMA 15:15	78.0/100	78.2/100	6.03	1.47	0.51	
BA/MMA 9:21	33.4/100	33.9/100	6.00	1.47	0.51	
BA/MMA 3:27	8.7/100	10.0/100	5.71	1.55	0.59	
methyl methacrylate (MMA)	100	100	5.54	1.6	0.64	1.67 [32]
BA/styrene 27:3	100/13.7	100/11.7	6.2	1.43	0.47	
BA/styrene 2:/9	100/52.9	100/46.3	6.89	1.28	0.32	
BA/styrene 15:15	81.1/100	87.0/100	6.93	1.27	0.32	
BA/styrene 9:21	34.8/100	41.2/100	7.06	1.25	0.29	
BA/styrene 3:27	9.0/100	10.4/100	7.09	1.24	0.28	
styrene	100	100	7.39	1.20	0.24	0.12[32]

[a] The molar ratio of the feed monomer was obtained by converting the feed monomer weight to the molar ratio. [b] The molar ratio of the monomer in the d_{001} space was obtained by integrating ^{1}H NMR spectrum peak areas: $-O-CH_3$ of MMA at 3.9 δ (single), $-O-CH_2-$ of BA at 4.1 δ (triple), and $CH_2=$ of styrene at 5.2 δ (double). [c] The gap size was calculated by subtracting the thickness of one MMT layer (0.96 nm) from the $d_{(001)}$ space obtained.[21] [d] The BA dipole moment value was calculated by using an energy-minimizing method of Chem Draw 6.0 at a minimum RNS gradient of 0.01.

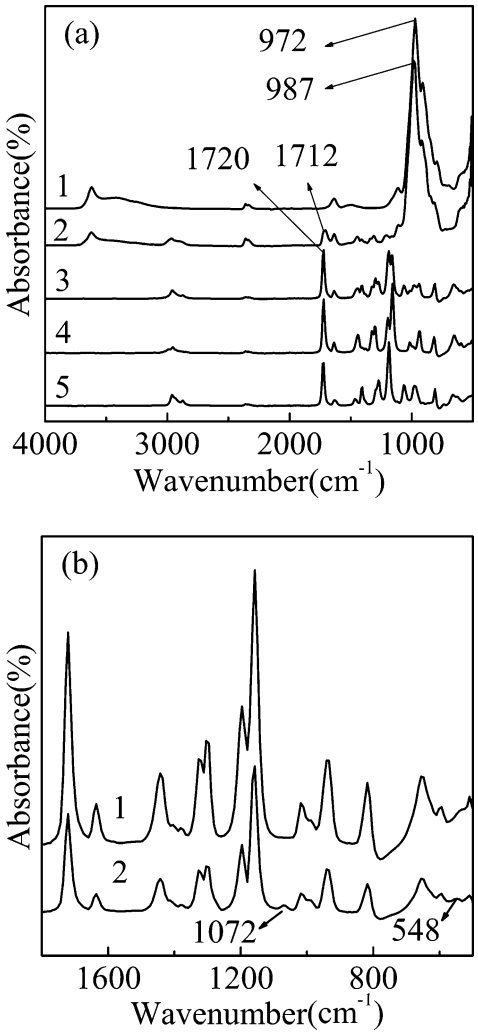

Figure 3. (a) FT-IR spectra of (trace 1) MMT; (trace 2) BA−MMA−MMT dispersion (the BA/MMA ratio is 15:15); (trace 3) BA−MMA comonomer (the BA/MMA ratio is 15:15); (trace 4) MMA, and (trace 5) BA. (b) FT-IR spectra of (trace 1) MMA, and (trace 2) spectrum after subtracting BA from the BA−MMA comonomer.

IPA, which have strong hydrogen-bonding groups, showed little suspended MMT.[18] On the other hand, the solvents with moderate or poor hydrogen-bonding groups precipitated MMT as soon as the agitation was finished. This phenomenon indicates that δ_h is important for dispersing natural MMT in solvents. It also indicates that the Hansen solubility parameters, rather than the total solubility parameters, can explain the interactions between the MMT and liquids.

Using the Hansen solubility parameters of liquids, we can explain how the interactions between organic liquids and MMT also affect the basal spacing expansion. Figure 1 (a) shows X-ray diffraction (XRD) peaks of MMT dispersed in liquids with strong or poor hydrogen bonding groups (δ_h). We omitted the XRD peak of water−MMT because of its high viscosity. The d_{001} spacing of liquid−MMT appears in the following order: MeOH (1.62 nm, 5.46°) > EtOH (1.57 nm, 5.64°) > IPA (1.40 nm, 6.33°) > *n*-hexane (1.21 nm, 7.30°) > toluene (1.19 nm, 7.41°) > benzene (1.19 nm, 7.44°). The liquids with high δ_h values expand the d_{001} spacing of MMT more than liquids with low δ_h values. Moreover, the spacing of natural MMT is strongly related to δ_h rather than δ_d because the liquids have almost the same δ_d values.

Experiments that use AN, BA, MMA, and styrene, which have almost the same δ_h values, explain the effect of δ_p on the basal spacing expansion. Figure 1(b) shows the basal spacing of MMT in the following order: BA (1.81 nm, 4.87°) > AN (1.66 nm, 5.30°) > MMA (1.60 nm, 5.54°) > styrene (1.20 nm, 7.39°). The monomers with high δ_p values enlarge the basal spacing of MMT. These results indicate that the δ_p and δ_h of liquids are the main parameters that affect the basal spacing expansion of MMT.

The monomer concentration is proportional to the degree of the basal spacing expansion. If the monomers inside the MMT particles take part in polymerization under a fixed amount of surfactant (AMPS), the degree of expansion produces different structures in the polymer−MMT nanocomposites. For polyacrylonitrile (PAN), PBA, and poly(MMA) (PMMA)−MMT nanocomposites, which have monomers with high δ_p values that enlarge the basal spacing of MMT before polymerization, we see no peaks within MMT composition ranges of 20 wt %. The absence of peaks indicates exfoliated structures. In

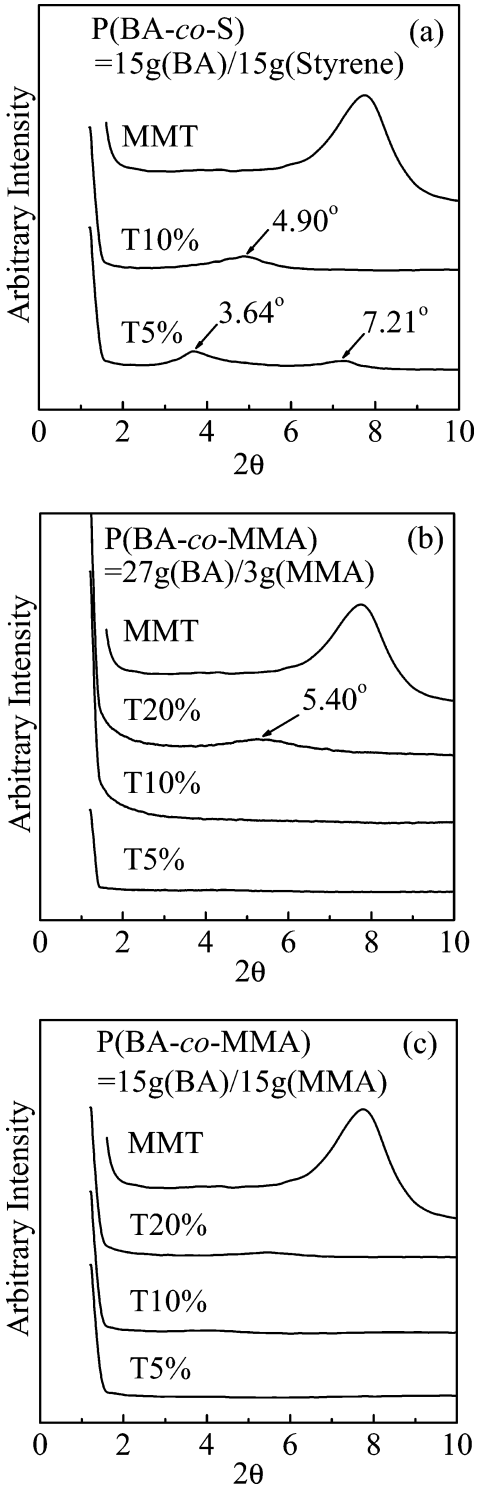

Figure 4. XRD patterns of polymer−MMT nanocomposites that contain various amounts of MMT loading: (a) P(BA-*co*-S)−MMT nanocomposites synthesized with a BA/styrene ratio of 15:15, (b) P(BA-*co*-MMA)−MMT nanocomposites synthesized with a BA/MMA ratio of 27:3, and (c) P(BA-*co*-MMA)−MMT nanocomposites synthesized with a BA/MMA ratio of 15:15. The percentage of T indicates the weight percentage of pristine MMT added to the monomer.

addition, styrene has a δ_t value similar to those of other monomers and a higher δ_d value than other monomers. However, styrene−MMT shows small basal spacing, whereas polystyrene (PS)−MMT nanocomposites show XRD peaks at 5.69° (3 wt %) and 5.96° (5 wt %). These

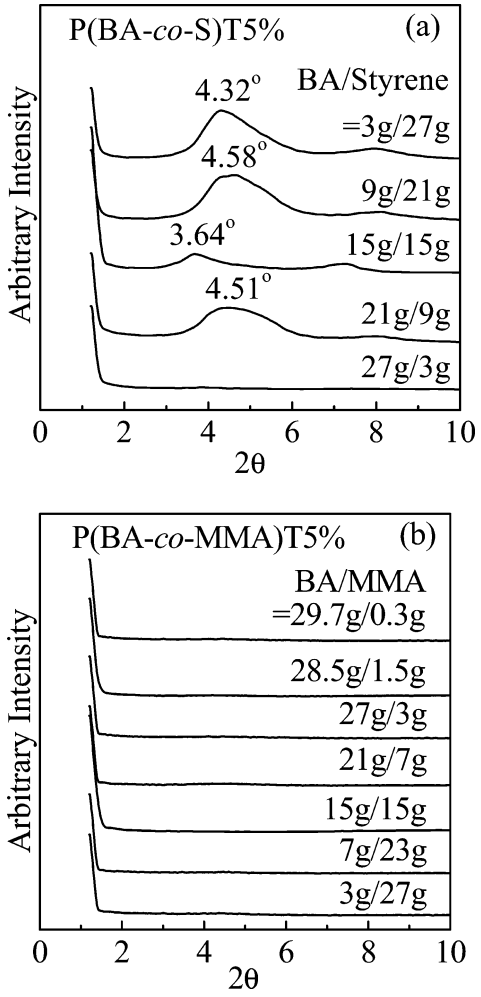

Figure 5. XRD patterns of (a) P(BA-*co*-S) and (b) P(BA-*co*-MMA)−MMT nanocomposites with various monomer ratios at 5 wt % of MMT loading.

results indicate intercalation. We can infer that the degree of basal spacing expansion by monomers reflects the structure of polymer−MMT nanocomposites.

The δ_p of monomers (polar liquids) and the δ_h of solvents strongly affect the basal spacing expansion. Because δ_p and δ_h are based on dipole−dipole interactions, monomer dipole moments can help explain MMT exfoliation.[32] To find the correlation between monomer dipole moments and the structures of polymer−MMT nanocomposites, we mixed the monomers—monomers have different dipole moment values and are miscible with each other.

As Figure 2(a) shows, the XRD peaks of the MMT dispersed in BA−styrene comonomers appear between the peaks of BA−MMT (4.87°) and styrene−MMT (7.39°). As the styrene content increases, the XRD peak shifts toward a high-angle position, approaching that of styrene−MMT. The BA−MMA−MMT is expected to have an XRD peak between the 2θ range of BA−MMT and MMA−MMT (5.54°) because the BA−MMA comonomers have dipole moment values between those of BA (2.31 D) and MMA (1.67 D). As the BA content in the comonomer increases, BA−MMA−MMT shows decreasing basal spacing until the weight ratio of BA to MMA is 27:3, as shown in Figure 2b. When the weight ratio of BA to MMA is below 27:3, the basal spacing increases to that of BA−MMT. This increase could be due to two

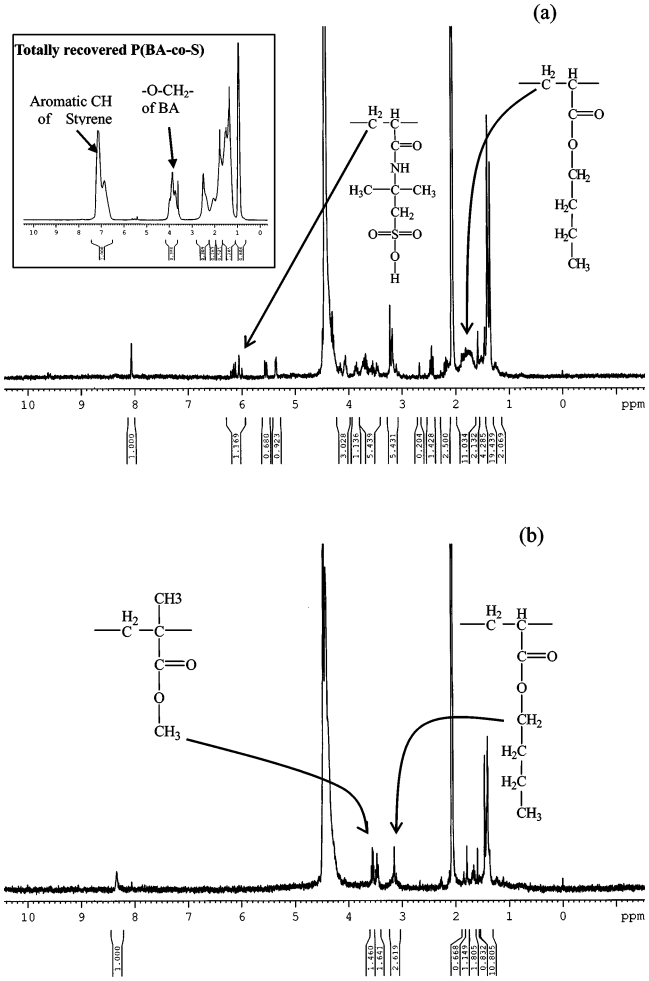

Figure 6. ^{1}H NMR spectra of (a) P(BA-*co*-S) recovered from P(BA-*co*-S)T10% and (b) P(BA-*co*-MMA) recovered from P(BA-*co*-MMA)T20% by reverse ion exchange with THF−LiCl, after a 5-day THF extraction with a Soxhlet extraction apparatus. A small ^{1}H NMR spectrum in the left side of (a) is the totally recovered P(BA-*co*-S) from P(BA-*co*-S)T10% by reverse ion exchange with THF−LiCl.

competitive interactions: the interaction between MMT and the mixed monomer, and the interaction between the two monomers.

We used FT-IR spectra to examine the peculiar basal spacing of BA−MMA−MMT. As shown in Figure 3a, trace 1, the absorbance bands around 3500 to 3400 cm^{-1} and at 1635 cm^{-1} were assigned as O−H stretching (hydration) and hydrated water deformation. These bands relate with the water content of MMT.[34] The wavenumbers and intensities of BA−MMA−MMT in Figure 3a, trace 2, are unchanged, indicating that the hydrated water in MMT rarely interacts with monomers and that the monomers do not vary the water content.

In contrast, the absorbance band for carbonyl stretching of the BA−MMA comonomer adsorbed on the MMT surface shifts to 1712 cm^{-1} from its clay-free state position (1720 cm^{-1}). Moreover, the Si−O stretching in MMT has an absorbance band at 987 cm^{-1}. As shown in Figure 3a, trace 2, this stretching reflects a shift from the dry-state frequency of 972 cm^{-1}. The FT-IR spectra

(34) Van Olphen, H.; Fripiat, J. J. *Data Handbook for Clay Materials and Other Nonmetallic Materials*; Pergamon Press: New York, 1979.

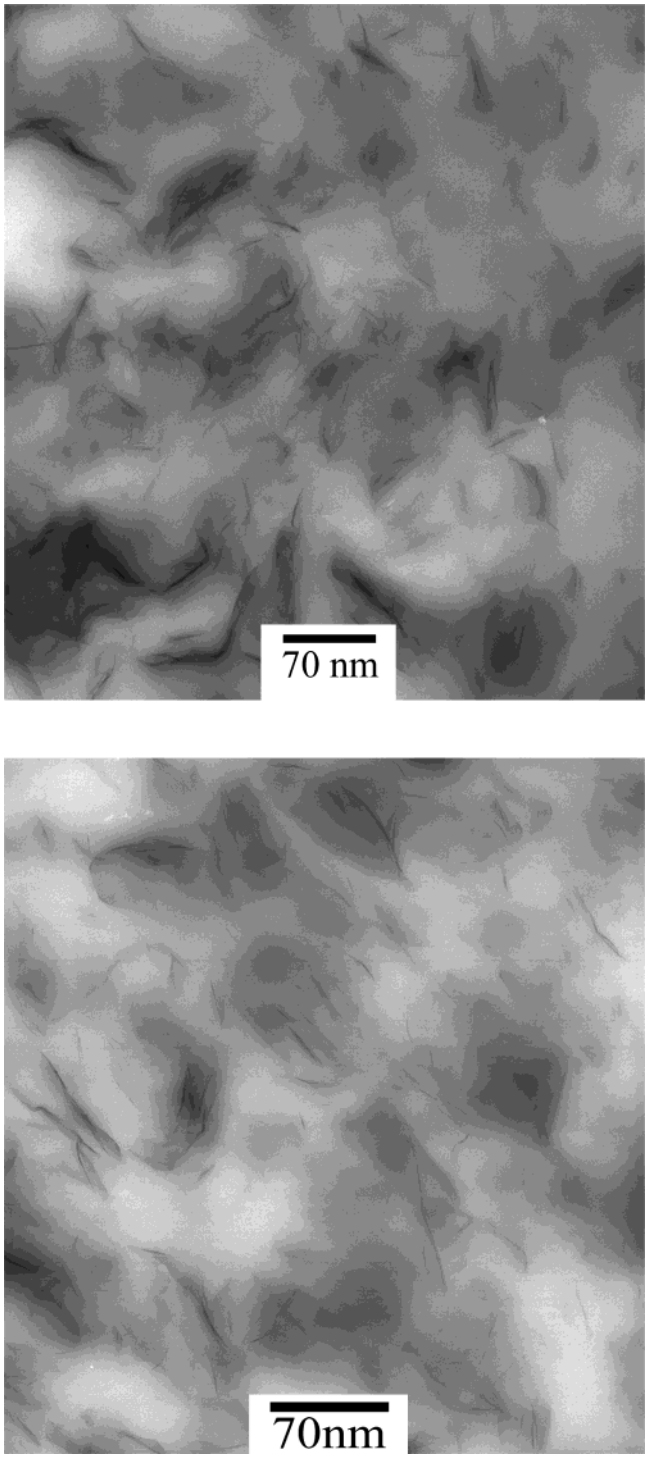

Figure 7. TEM micrographs of (a) a PBA−MMT nanocomposite and (b) a P(BA-*co*-MMA)−MMT nanocomposite containing 5 wt % of clay.

illustrate that the BA−MMA comonomer and MMT interact with carbonyl groups and silicone-oxides, which are based on the dipole−dipole interaction. After subtracting the BA spectrum from the spectrum of the BA−MMA comonomer, new absorbance peaks appeared at 1072 and 548 cm^{-1}, as shown in Figure 3b, trace 2. These two peaks indicate that BA and MMA interact with each other through the dipole−dipole interaction.

Table 2 lists the monomer dipole moments and the basal spacing of MMT. The basal spacing of MMT changes according to the monomer dipole moment

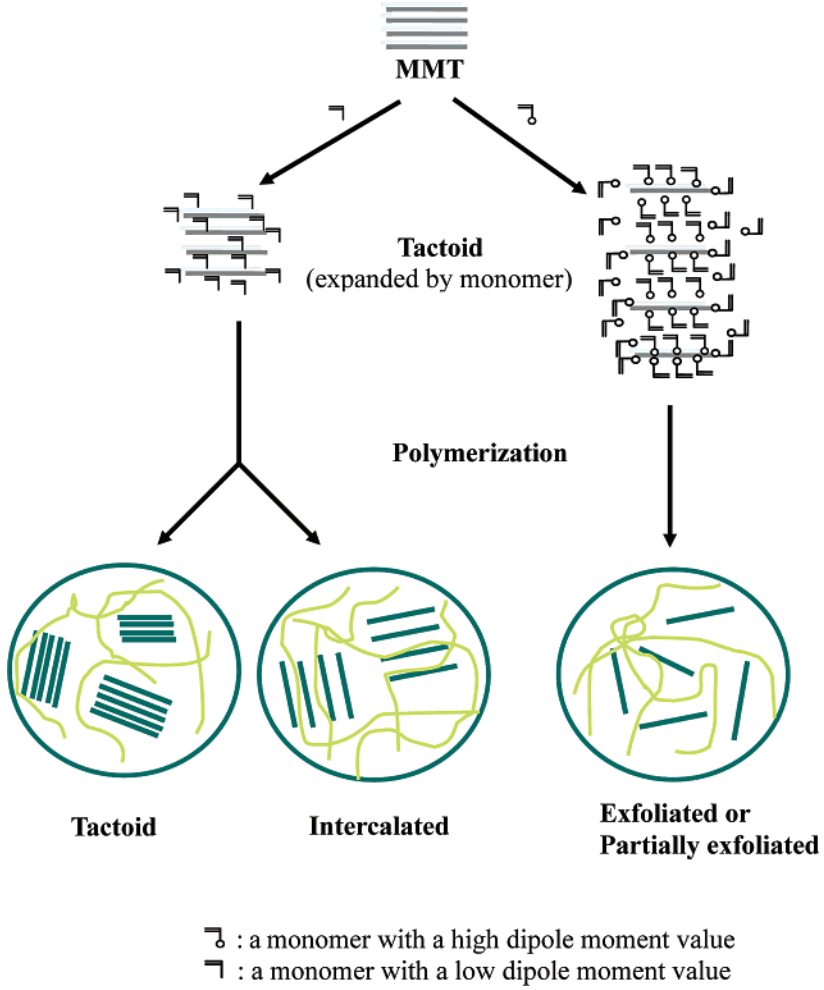

Figure 8. Schematic representation showing the correlation between the basal spacing expansion by monomers and the structure of polymer−MMT nanocomposites.

values. The BA−MMA comonomers in the basal spacing show almost the same ratio as the feed monomer ratio, though the BA−styrene comonomers show a smaller styrene portion than the feed monomer ratio. This reduction indicates that styrene is less interactive with the clay layer than BA or MMA.

For the copolymer−MMT nanocomposites, we conducted the experiments in two ways: we varied the MMT loading in the copolymer−MMT nanocomposites; and we varied the monomer composition at an MMT loading of 5 wt %. The poly(BA-*co*-styrene)−MMT nanocomposites were synthesized with BA and styrene at a weight ratio of 15:15. Figure 4a shows the intercalated states. XRD peaks for P(BA-*co*-S)T10% and T5% appear at 4.90° and 3.64°, and the d_{001} spacing for the peaks is 2.00 and 2.70 nm, respectively. The percentage symbol next to T indicates the MMT percent relative to the monomer weight.

We synthesized P(BA-*co*-MMA)−MMT nanocomposites with BA and MMA at a weight ratio of 27:3. No XRD peaks occurred up to an MMT loading of 10 wt %, though, in Figure 4b, the nanocomposite shows an XRD peak at 5.40° with an MMT loading of 20 wt %. As shown in Figure 4c, the other nanocomposites that were synthesized with BA and MMA at a weight ratio of 15:15 show no XRD peaks within an MMT loading of 20 wt %. As mentioned earlier, a BA−MMA comonomer with a weight ratio of 27:3 shows a narrower MMT basal spacing than one with a ratio of 15:15g before polymerization. These XRD peaks illustrate that the basal spacing expansion correlates with the structures of polymer−MMT nanocomposites.

Figure 5a shows that all P(BA-*co*-S)−MMT nanocomposites synthesized with 5 wt % MMT have intercalated structures, except for the nanocomposite synthesized with BA and styrene at a weight ratio of 27:3. The P(BA-*co*-MMA)−MMT nanocomposites most likely show no XRD peaks within the monomer ratios of Figure 5b because MMA has a higher dipole moment value than styrene. The XRD peaks show that the monomer dipole moments affect the basal spacing expansion, and that the expansion reflects the nanocomposite structures.

We used the ^{1}H NMR spectra of two nanocomposites to examine the interactions between MMT and monomers. After synthesizing bulk P(BA-*co*-S) copolymers with BA and styrene at a ratio of 15:15, we used THF extraction to remove them from P(BA-*co*-S)T10% and we used a reverse-ion-exchange method to obtain the copolymers end-tethered on MMT.[11]

Figure 6a shows the results. The NMR solvent peaks appeared at 4.6 δ (water) and 2.05 δ (acetone). The characteristic peaks for determining the BA/styrene/MPS ratio in MMT are as follows: the main-chain methylene protons (1.6−2.0 δ) of BA, the phenyl protons

(6.8−7.4 δ) of styrene, and the methine protons (6.0−6.1 δ) of AMPS. We found that the molar ratio was about 4.5:0:1 (BA/styrene/AMPS). The styrene ratio was much smaller than that of a totally recovered P(BA-*co*-S) copolymer from the nanocomposite, as the BA/styrene ratio was 95:100. We calculated the BA/styrene ratio by using the peak areas between 3.6 and 4.2 δ (BA, $-O-CH_2-$) and between 6.8 and 7.4 δ (styrene, aromatic C−H).

By using peak areas of the side-chain methylene protons ($-O-CH_2-$, 3.1−3.2 δ) of BA and the methoxy protons ($-O-CH_3$, 3.4−3.6 δ) of MMA, as given in Figure 6b, the BA/MMA ratio of an end-tethered copolymer separated from P(BA-*co*-MMA)T20% by the reverse-ion-exchange method was about 1:1 (BA/MMA). This ratio is identical to the feed monomer ratio: the BA/MMA ratio is 15:15. As expected from the monomer dipole moment values, styrene has less interaction with MMT than BA or MMA.

The TEM image in Figure 7 shows the dispersed states of MMT in PBAT5% and P(BA-*co*-MMA)T5%. The MMT layers appear as dark strips but the polymer matrix appears as a white domain. The individual MMT layers are dispersed uniformly in the polymer matrixes.

Two conditions are required to exfoliate MMT layers in polymer matrixes (refer to Figure 8). The first condition is that the interlayer spaces of MMT must be expanded; this expansion produces a favorable environment for the polymerization in the spaces. Monomers and initiators easily penetrate the interlayer spaces during the aqueous phase. The second condition is that the preadsorbed monomers attract reactants to the interlayer spaces during the polymerization. The polymerization rate for the emulsion system correlates with the first order of monomer concentration and the number of growing particles.[33] The more monomers in the basal spacing, the faster the polymerization rate.

Conclusion

To analyze the dispersion states and the basal spacing expansion of natural MMT in organic liquids, we used the Hansen solubility parameters. The hydrogen components (δ_h) and the polar components (δ_p) of liquids are the primary parameters for the dispersion states and for the basal spacing expansion. The degree of expansion by monomers reflects the structure of polymer−MMT nanocomposites: large basal spacing produces exfoliated structures and small basal spacing produces interacted structures. The correlation between the basal spacing expansion and the structure of polymer−MMT nanocomposites is reasonable because the polymerization rates depend on the monomer concentrations. Because δ_h and δ_p both involve dipole−dipole interactions, monomer dipole moments are associated with the basal spacing expansion that is related to the structure of polymer−MMT nanocomposites. Furthermore, because monomers with high dipole moment values enlarge the basal spacing, the monomer dipole moments are a useful tool for predicting the structure of the polymer−MMT nanocomposites prepared via in situ polymerization methods.

In this article, we explain how natural MMT interacts with organic liquids through dipole−dipole interactions. We also explain how monomer dipole moments affect the basal spacing expansion that is related to the degree in which MMT layers are distributed in polymer matrixes.

Acknowledgment. We express their sincere thanks to KOSEF (Korea Science and Engineering Foundation), to CAFPoly (Center for Advanced Functional Polymers), and to the BK 21 program for their financial support.

CM0348601